Noise Robustness Analysis of Sparse Representation based Classification Method for Non-stationary EEG Signal Classification

Younghak Shin[1], Seungchan Lee[1], Minkyu Ahn[2], Hohyun Cho[1], Sung Chan Jun[1], and Heung-No Lee[1*]

[1]*School of Information and Communications, Gwangju Institute of Science and Technology (GIST), Gwangju, Republic of Korea*
[2]*Department of Neuroscience, Brown University, Rhode Island, USA*
E-mail: heungno@gist.ac.kr

ABSTRACT

In the electroencephalogram (EEG)-based brain-computer interface (BCI) systems, classification is an important signal processing step to control external devices using brain activity. However, scalp-recorded EEG signals have inherent non-stationary characteristics; thus, the classification performance is deteriorated by changing the background activity of the EEG during the BCI experiment. Recently, the sparse representation-based classification (SRC) method has shown a robust classification performance in many pattern recognition fields including BCI. In this study, we aim to analyze noise robustness of the SRC method to evaluate the capability of the SRC for non-stationary EEG signal classification. For this purpose, we generate noisy test signals by adding a noise source such as random Gaussian and scalp-recorded background noise into the original motor imagery based EEG signals. Using the noisy test signals and real online-experimental dataset, we compare the classification performance of the SRC and support vector machine (SVM). Furthermore, we analyze the unique classification mechanism of the SRC. We observed that the SRC method provided better classification accuracy and noise robustness compared with the SVM method. In addition, the SRC has an inherent adaptive classification mechanism that makes it suitable for time-varying EEG signal classification for online BCI systems.

Keywords: Brain-computer interface (BCI), Electroencephalogram (EEG), Sparse representation based classification (SRC), Common spatial pattern (CSP), Non-stationarity.

1. Introduction

Brain-computer interface (BCI) systems provide a new communication and control channel between people and external devices [1]. In these systems, users can control an external device using their intention or imagination without making any real muscle movement. Therefore, these systems are very helpful for people who are suffering from severe motor diseases. The electroencephalogram (EEG) is widely used for measuring brain signals in BCI systems because of its low cost, no space restriction, and high temporal resolution compared with other equipment such as functional magnetic resonance imaging (fMRI) and magneto encephalogram (MEG) [2,3]. However, scalp-recorded EEG signals are very sensitive to noise. In particular, in the case of motor imagery based BCI, which uses induced EEG signals while the subject imagines limb movements [2,3], the instability of imagery task, non-stationarity of signals, and lack of concentration are among main obstacles to effectively process the EEG signals. In addition, it is difficult to collect a large set of training samples because of the subject's fatigue. The raw EEG signals are associated with high dimension owing to the large number of EEG channels; hence, it is difficult to collect volume of data samples that are large enough for good training. Therefore, EEG signal processing is very important and many research efforts have been focused on this issue [5–7].

The signal processing steps in BCI can be categorized as preprocessing, feature extraction, and classification. In the preprocessing step, the artifact detection and rejection are conducted. The purpose of feature extraction is to make a meaningful low-dimensional data, i.e., a feature vector, from the original high-dimensional data. This feature vector should be distinguishable for different classes. Typically, the feature extraction is performed using a dimensionality reduction method. The principal component analysis (PCA), independent component analysis (ICA), and common spatial pattern (CSP) are popular methods for dimensionality reduction in the motor imagery based BCI systems [7,20].

Another important signal processing step is classification. In the BCI systems, the purpose of classification is to translate the extracted feature of a user's intention into a computer command, which can then be used to control external devices. Typically, this translation is done using the classification algorithms, which are adopted from pattern recognition area. Frequently used classification methods in the EEG based BCI systems are linear classifiers such as linear discriminant analysis (LDA) and support vector machine (SVM) [6]. In many BCI studies, the SVM has been recognized as a robust classification method with generalization ability and has shown to provide the best classification results [6,14,15].

Recently, in the field of pattern recognition, the concept of sparse representation based classification, namely SRC, has been introduced [8]. The basic idea of SRC is to parsimoniously represent a test signal $\mathbf{y}$ via the so-called sparsification step, i.e., $\mathbf{y} = \mathbf{A}\mathbf{x}$, where $\mathbf{A}$ is a dictionary whose columns are a collection of training signals. This sparsification step leads to the representation of the test signal $\mathbf{y}$ with the training signals from the same class predominantly. The L1 minimization algorithm is employed to perform the sparse representation of the test signal with a given set of training signals.

The robust classification performance of the SRC framework has been shown in various applications such as face recognition [9,12,13,24], digit classification [8], and speech recognition [10]. Particularly, in [9], Yang *et al.* presented that SRC obtains robust face recognition performance for occlusion and corruption on facial images. In addition, SRC has been successfully applied to the EEG based BCI application [11] and EEG based vigilance detection [28]. However, in the EEG signal classification, SRC is rarely studied. The previous SRC study for the motor imagery

based EEG signal classification focused on algorithm construction and evaluated the classification performance compared with a conventional classifier such as LDA in [11]. To the best of our knowledge, there has been no literature to systematically evaluate the noise robustness and classification characteristics of SRC for the scalp recorded EEG signals.

It is well known that EEG signals are non-stationary. The non-stationarity can be observed during the change in alertness and wakefulness, eye blinking, and in the event-related potential (ERP) and evoked potential (EP) such as motor imagery signals [32]. Because of the non-stationarity of the EEG, we can observe that the test feature positions vary from the original training feature positions in the feature space [6,16]. This is one of the major obstacles in EEG signal classification. Thus, a classifier that is optimized for a particular training data may not work for online BCI with a new test data.

Recently, extensive research efforts have been devoted to overcome the non-stationary issue in the motor imagery based EEG classification. In [38–40], robust feature extraction methods were proposed for common spatial pattern (CSP), which is the most widely used technique for feature extraction in the motor imagery BCI. In the classification stage, supervised and un-supervised adaptive classification schemes were studied for the conventional LDA and SVM methods [16,27,41].

In this study, our aim is to evaluate the robustness of SRC for non-stationary EEG signal classification. First, we compare the classification performance, i.e., classification accuracy and computation time, of the SRC with SVM, which has been known as the state of the art classifier in many studies. Second, we evaluate the noise robustness of the SRC and SVM methods. For this purpose, we generate noisy test signals which have different feature distribution with original test signals. The noisy test signals are generated with the addition of random Gaussian noise and scalp recorded background EEG signal into the original test signal. Then, we assess the noise robustness of both SRC and SVM methods. Third, in addition to the simple performance comparison, we examine working mechanism of SRC by analyzing advantages and disadvantages as the role of classifier compared with the conventional SVM. Moreover, we discuss why SRC outperforms SVM for the noisy test signal. Finally, we evaluate the SRC method using an online experimental dataset where non-stationarity occurs from training to testing sessions. Our work is intended to provide evaluation and analysis of SRC to researchers who want to apply the SRC framework to non-stationary EEG signal classification.

This paper is organized as follows: In section 2, the experiment and EEG signal processing methods such as feature extraction and classification are described. In addition, noise robustness analysis method is explained in this section. Section 3 shows the experimental results. In section 4, discussions and analysis are provided. Finally, we conclude this paper in section 5.

2. Methods

2.1. Experiment

In this study, to evaluate and analyze the SCR method, we perform two-class EEG based motor imagery experiment. Twenty healthy subjects (11 male and 9 female subjects whose average age is 24.05±3.76) participated in this experiment. Therefore, we collected 20 motor imagery datasets. Each dataset contains EEG signals generated from the left and right hand motor imagery experiment. Experiment included five runs. One run consisted of 20 trials for each class. Thus, the total number of trials was 100 for each instruction (class).

Fig. 1 shows a single trial experimental paradigm of our motor imagery experiment. Cue line indicates the starting point of motor imagery. One trial consisted of 4–6 sec of resting time period and 3 sec of imagery time period. In the resting period, a blank screen appeared on the monitor. The resting time was randomly selected in the range of 4 to 6 sec. In the imagery period, one of the motor imagery instructions was represented at the center of the screen, then subjects imagined their left or right hand movements for tasks such as grasping and releasing hand. In each trial, instruction was randomly selected from the left and right hand class.

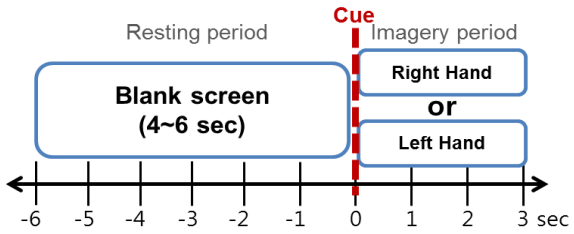

Fig. 1. Single trial time procedure of motor imagery experiment.

In addition, we recorded resting state EEG signals for each subject to estimate the subject-specific background noise. In this recording, subjects were instructed to open their eyes for 60 sec without any experimental task.

These experimental datasets were recorded by an active electrode cap. We used Active Two EEG measurement system made by Biosemi, Inc. The sampling rate for these datasets was 512 samples per second, and the number of EEG channels was 64. The channel positions were selected from the international 10/20 standard.

2.2. Preprocessing and Feature Extraction

Preprocessing and feature extraction steps are common to both SRC and SVM classification algorithms. Using the motor imagery dataset obtained from each subject, we perform the data preprocessing. Before preprocessing, raw EEG signals are segmented. After an instruction (left or right hand) appears on the screen, the time samples from 1 to 2 sec were collected for all trial data. We apply the band pass filter to the trial data to eliminate the frequencies that are not related to motor imagery signals. In this study, sensorimotor rhythm, 8 to 15 Hz, is used for band pass filtering [11]. For fair comparison of the classification performance, we fixed the time and frequency range for all subjects. Then, we reduce the dimension of EEG signal using the common spatial pattern (CSP) filtering, which is a widely used feature selection method for motor imagery based BCI systems [5,11,20]. CSP filters maximize the variance of the spatially filtered signal under one class condition while minimizing it for the other class condition. The CSP filtering algorithm finds the filters, $\mathbf{W} \in \mathbb{R}^{C \times C} = [\mathbf{w}_1, \mathbf{w}_2, \cdots, \mathbf{w}_C]$ which transforms the EEG data $\mathbf{X} \in \mathbb{R}^{C \times S}$ (C and S denote the number of EEG channels and time samples) into a spatially filtered space: $\mathbf{X}_{CSP} = \mathbf{W}^T \cdot \mathbf{X}$. Generally, W is computed by simultaneous diagonalization of the covariance matrices, Σ_1 and Σ_2 , of the two classes of data. This is equivalent to solving the generalized eigenvalue problem, i.e., $\Sigma_1 \mathbf{w} = \lambda \Sigma_2 \mathbf{w}$, where λ is the eigenvalue. In practice, the first and last n columns of the $\mathbf{W}$ correspond to the n largest and n smallest eigenvalues that are used for CSP filtering. However, the optimal number of CSP filters, $m = 2n$, which shows the maximum classification accuracy varies and has

to be chosen empirically [20]. After CSP filtering, for each CSP filtered trial, we compute the frequency power of sensorimotor rhythm (8–15 Hz) which is the widely used band power (BP) feature in motor imagery based BCI classification [6,11]. Various feature types including BP, AR (autoregressive) [6], and functional connectivity [42] can be used for motor imagery classification. However, in this study, we focus on the evaluation of classification methods using a common feature type.

2.3. Classification Methods

2.3.1. Sparse Representation based EEG Signal Classification

The SRC framework was introduced to the EEG based motor imagery BCI application in [11]. There, the SRC method showed a better classification accuracy over the conventional LDA method.

In the SRC method, dictionary is first formed using the processed training feature. Let $\mathbf{A}_i = [\mathbf{a}_{i,1}, \mathbf{a}_{i,2}, ..., \mathbf{a}_{i,N_t}]$ be the class-dictionary for classes $i = L$ and R where L and R represent class information of left hand and right hand motor imagery respectively, and N_t is the total number of training trials, i.e., $N_t = 99$ for each class in this study. Then, the final dictionary $\mathbf{A}$ is formed by $\mathbf{A} := [\mathbf{A}_L; \mathbf{A}_R]$. Each column vector $\mathbf{a} \in \mathbb{R}^{m \times 1}$ where m is the number of applied CSP filters. In this study, we used 64 EEG channels; thus, m is varied from 2 to 64. Each entry of $\mathbf{a}$ is obtained by computing the frequency power of sensorimotor rhythm after the CSP filtering. Let $\mathbf{y}$ denote a testing feature with the same dimension as $\mathbf{a}$.

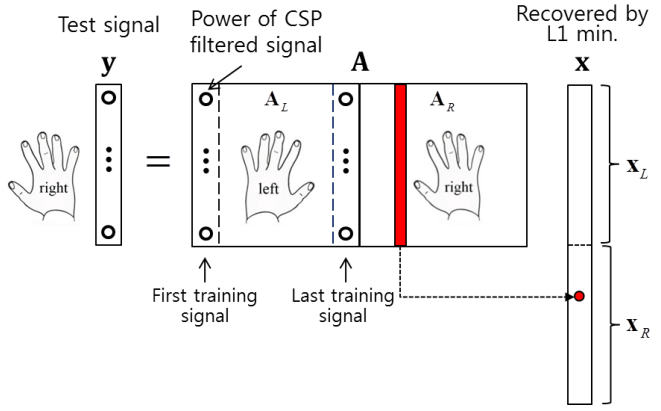

Fig. 2. Dictionary design and linear sparse representation model for SRC.

Fig. 2 shows the formed dictionary $\mathbf{A}$ and model of sparse representation for motor imagery based EEG signals. In this example, a certain test feature $\mathbf{y}$ of the right hand class can be sparsely represented with a linear combination of training feature of the right hand class. This is represented by the nonzero scalar coefficients $\mathbf{x}$ in the position of corresponding class.

The SRC method can be summarized in the following two steps. The first step is to sparsely represent $\mathbf{y}$ using $\mathbf{A}$ via L1 norm minimization. This step is the sparsification step:

$$\min_{\mathbf{x}} \|\mathbf{x}\|_1 \text{ subject to } \mathbf{y} = \mathbf{A}\mathbf{x} \tag{1}$$

where $\mathbf{x}$ is a scalar coefficient vector and $\mathbf{A} \in \mathbb{R}^{m \times n}$ is the dictionary.

Note that the linear system in Eq. (1) is under-determined. The literature of compressive sensing (CS) shows that the L1 minimization algorithm can solve this optimization problem in polynomial time [17,18,21].

The second step is to classify the test signal via minimum residual. This step is the identification step:

$$\text{class}(\mathbf{y}) = \min_i r_i(\mathbf{y}) \tag{2}$$

where $r_i(\mathbf{y}) := \|\mathbf{y} - \mathbf{A}_i \mathbf{x}_i\|_2$, $\mathbf{x}_i$ is the scalar coefficient vector corresponding to the class *i*.

2.3.2. Support Vector Machine

SVM is a well-known classification method in the area of pattern recognition and machine learning. In the BCI field, the SVM has shown a robust classification performance in many experimental studies [6,14,15]. SVM is recognized for its excellent generalization performance, i.e., small error rate for test data. This property is achieved through the idea of margin maximization. As shown in Fig. 3, the margin *d* is twice the distance between the support vector (the black and white circles that are on the dashed line) and the decision hyperplane. The hyperplane can be described by a weight vector $\mathbf{w}$ and a bias b . The SVM finds the decision hyperplane by solving the following optimization problem [19]:

$$\begin{aligned} &\text{minimize} \quad \frac{1}{2}\|\mathbf{w}\|^2 + C\sum_n \xi_n, \\ &\text{subject to} \quad t_n(\mathbf{w}^T \Phi(\mathbf{y}_n) + b) \geq 1 - \xi_n \\ &\qquad\qquad \xi_n \geq 0, n = 1, ..., N \end{aligned} \tag{3}$$

where $\mathbf{y}_n$ is the training feature vector, $t_n \in \{+1, -1\}$ is the class information and n indicates the training trial number. To consider the training error, a slack variable ξ and a regularization parameter C are included [19]. Using ξ , we can consider the training error which is positioned inside the support vectors. C is a user defined regularization parameter to control the importance between the maximum margin and the training error.

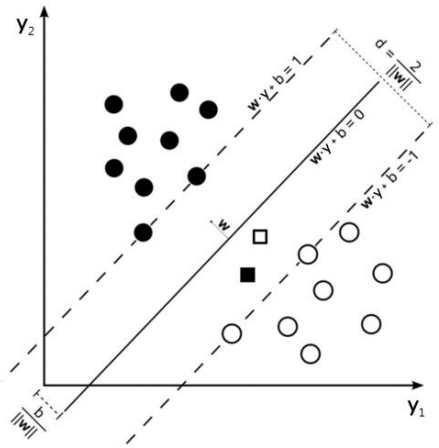

Fig. 3. The main idea of SVM. The SVM algorithm tries to find the decision hyperplane, which has the maximum margin d.

In the SVM optimization problem, mapping function $\Phi(\cdot)$ can be used to map an inseparable feature vector onto a higher-dimensional space using a kernel function $K(\mathbf{x}, \mathbf{y})$. In BCI research, the Radial Basis Function (RBF) kernel (4) is widely used and has shown robust classification performance [6,15]:

$$K(\mathbf{x}, \mathbf{y}) = \exp\left(\frac{-\|x - y\|^2}{2\sigma^2}\right) \tag{4}$$

Therefore, in this study, we consider a linear SVM and an RBF kernel based SVM for comparison of the classification performance with the SRC method. For both SVM algorithms, we use the MATLAB Bioinformatics Toolbox (SVMtrain) [23].

In the SVM algorithm, selection of parameters is important to obtain the robust performance. We optimize the regularization parameter C in (3) for linear SVM and kernel parameter σ in (4) with combination of C for RBF SVM. We adopt a coarse grid search method using cross-validation to find optimal parameters that provide the best classification accuracy [25]. In the exhaustive coarse grid search, we first find a better region on the loose grid, then fine grid search on that region is conducted. For two parameters C and σ, we set the same grid sequence as follows: C and $\sigma = [10^{-3}, 10^{-2}, 10^{-1}, 10^{0}, 10^{1}, 10^{2}, 10^{3}]$. Then, for the best region, we optimize the parameters using a fine tuning.

2.4. Noise Robustness Analysis Method

In this study, we aim to evaluate the noise robustness of the SRC and SVM classification methods when our test data is contaminated by an additive random Gaussian noise and scalp recorded background noise. The ultimate goal of this evaluation is to assess the classification performance of both methods for non-stationary EEG signal. As it is known, EEG signals have inherent non-stationary characteristics. Therefore, BCI features vary from training sessions to test sessions during a BCI experiment [6,16,38]. There are many reasons to change EEG signals in the motor imagery task such as physical and mental drifts, misalignment of sensors, and task–irrelevant background activity [33,38]. During the imagery period in the motor imagery experiment, when we assume subjects exclusively perform motor imagery task, the task-irrelevant background activity can be the main reason for a change in EEG signals [16,38]. In [36–37], authors also considered the resting state signal as task-irrelevant noise in the motor imagery task. In addition, in [16], it was showed that EEG signals were changed from training to online testing sessions in feature space by changing the background activity. Therefore, in this context, we aim to model the modified noisy test signals by adding background activity estimated by the resting state recording into the original test signal.

For robustness analysis, we generate the modified test data by introducing two different noise sources such as white Gaussian and background noise into the original test data. Each noise source signal is separately applied to the EEG test data. Thus, we evaluate the classification performance of both classifiers for two types of noise corrupted test data. In result section, we show the position shift in the noisy test feature that is generated by the background noise (see Fig 10).

Fig. 4 shows the generation concept of the polluted noisy test data using one noise source. In the online BCI experiment, the power of EEG test data varies. Therefore, to evaluate the noise robustness of the classifiers systematically, we generate five different noisy test data with various SNR levels. Thus, we control the noise power of each noise source in five levels.

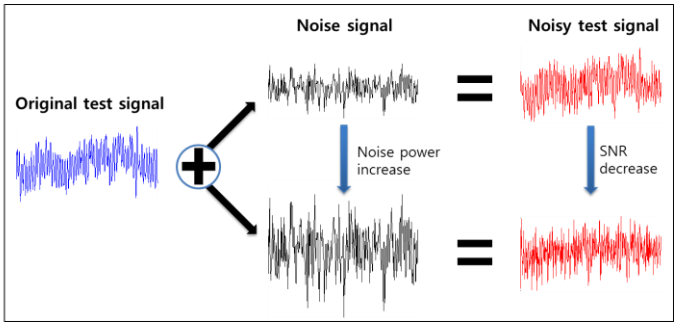

Fig. 4. Noisy test signal generation using different power of noise signal.

For the Gaussian noise, we control the noise power by varying the standard deviation of Gaussian distribution. For the background noise, we use a scale factor α to control the noise power as follows:

$$\text{polluted test signal} = \text{test signal} + \alpha(\text{resting noise}) \qquad (5)$$

For each subject's dataset, the classification performance of the SRC and SVM methods is evaluated using both types of noisy test data.

Random Gaussian noise is artificially generated by m-dimensional Gaussian distribution, i.e., $N_m(\mu, \sigma^2)$ where μ and σ^2 are the mean and variance. We use a MATLAB built-in function to generate the zero mean Gaussian distribution with different standard deviation σ. To make polluted EEG test data by Gaussian noise, we generate the same dimension of Gaussian noise to the segmented EEG signal, i.e., noise dimension is 64 by 512. We also apply the band pass filter to the generated Gaussian noise with 8–15 Hz cutoff frequency, which is used in the preprocessing of EEG signal.

Subject-specific background noise is measured by the EEG recording of the resting state. In this recording, subject is instructed to just open their eyes without any task for one minute. We apply the band pass filter to the recorded resting state signal. To make polluted EEG test data by background noise, we collect one-second time samples (512 samples) from the resting state signal. In this study, both classifiers are evaluated using 100 test trials. Therefore, we generate 100 noise signals using the moving window from the total resting state signal. The size of the moving window is 256 samples (0.5 second).

To evaluate and compare the classification accuracy of the SRC and SVM methods, we use the leave-one-out (LOO) cross-validation, which is useful for increasing the number of independent classification tests with a given set of limited data trials [22]. Thus, one trial out of 100 training trials is selected as the test trial, and the remaining trials are used as the training trials. This test is repeated for 100 times with different combination of training and test trials. To obtain noisy test trials, we apply 100 different noise signals for each noise source into the 100 test trials acquired from LOO cross-validation. Therefore, we have 100 noisy test trials for each Gaussian and background noise. In this study, we calculate the classification accuracy as follows:

$$\text{Accuracy}(\%) = \frac{\text{the number of correct test trials}}{\text{the number of total test trials}} \times 100 \qquad (6)$$

3. Results

3.1. Comparison of Classification Results

First, we evaluate the classification accuracy of the SRC and SVM methods for the original experimental datasets that are not contaminated by noise sources. Fig. 5 shows the comparison result of the classification accuracy for the SRC, linear SVM, and RBF SVM. For each subject, we computed the classification accuracy (in %) using the LOO cross-validation. We used 18 CSP filters for both classification methods, which are determined heuristically (see Fig. 6).

In Fig. 5, we observe that SRC achieves competitive classification accuracy over both linear and RBF kernel-based SVM. The classification accuracy of SRC was found to be better than linear SVM for 15 subjects and RBF SVM for 14 subjects over 20 subjects. In addition, the mean difference of the classification accuracy between the SRC and both SVM methods was statistically significant using the paired t-test ($p < 0.01$).

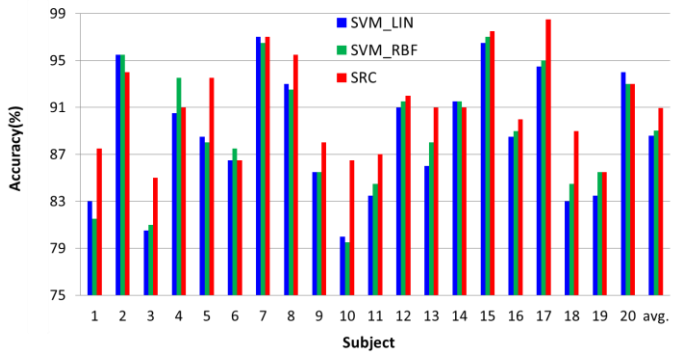

Fig. 5. Comparison of classification accuracy for the linear SVM, RBF kernel SVM, and SRC method using 20 non-noisy experimental datasets.

Moreover, we investigated the impact of varying the feature dimension on the non-noisy classification performance in each method (see Fig. 6). In this study, we used the CSP filtering as a feature selection method. The number of CSP filters (feature dimension) was varied from 2 to 64. Usually, the optimal number of CSP filters, which showed the maximum classification accuracy was chosen empirically. However, the optimal number of CSP filters was different depending on the classification method and dataset. Therefore, we evaluated the classification performance of each classification method when the feature dimension was varied. Fig. 6 shows the average classification accuracy over all subjects when the number of feature dimensions *m* was varied from 2 to 64. We found that the classification accuracy of SRC method consistently outperformed the linear and RBF kernel based SVM methods regardless of their feature dimension. There was not much difference in the classification accuracy between the SVM methods. However, the RBF SVM showed a better classification accuracy when the number of CSP filters was over 18.

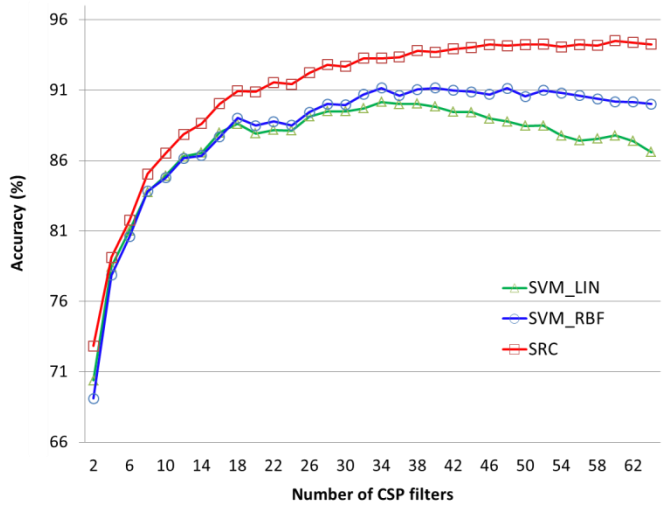

Fig. 6. Average classification accuracy over 20 non-noisy datasets when the number of CSP filters (feature dimension) is varied from 2 to 64.

We used the fixed 18 CSP filters for all classification methods that are shown in Fig. 5. However, the results in Fig. 6 shows that this number was not optimal for certain classification methods. When we used more CSP filters, the difference in the classification accuracy between the SRC and SVM methods was increased.

3.2. Classification Results for Noise Robustness

In this section, we evaluate noise robustness of the RBF kernel based SVM and SRC methods. For the noise robustness analysis, we used polluted test signals that were generated by adding two noise sources, i.e., white Gaussian noise and background noise, into the original test signal as mentioned in section 2.4.

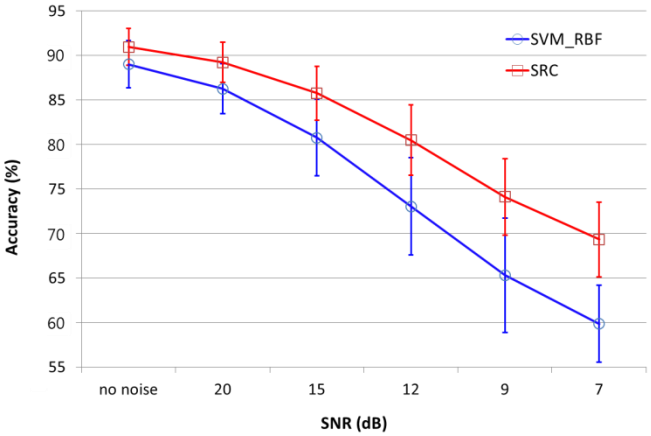

Fig. 7. Comparison of the average classification accuracy over 20 subjects. Average classification accuracy for Gaussian noise is represented as a function of SNR. Vertical line indicates the standard deviation of the accuracy for each SNR.

Fig. 7 shows the noise robustness results of the SRC and RBF kernel based SVM methods for the Gaussian noise. The average classification accuracy over all subjects was assessed when the noise power was varied. For the Gaussian noise, we controlled the noise power by changing the standard deviation, and the SNR was computed for different noise powers. In this study, SNR computation was defined as follows:

$$\mathrm{SNR(dB)} = 10\log_{10}\left(\frac{P_S}{P_N}\right) \tag{7}$$

where P_S and P_N indicate the signal and noise power, respectively. For the SNR computation, we investigated the average SNR over all the channels and subjects. As shown in Fig. 7, we found that the classification accuracy of SRC was higher than that of the RBF SVM for all SNR cases. The difference in the classification accuracy between the SRC and RBF SVM was increased with the SNR increase.

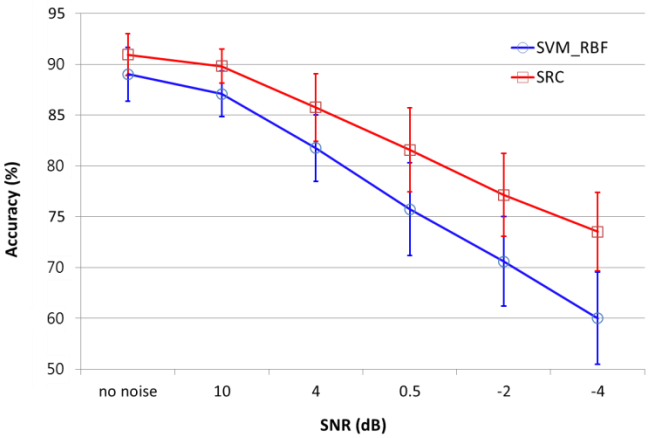

Fig. 8. Comparison of the average classification accuracy over 20 subjects. Average classification accuracy for background noise is represented as a function of SNR.

Similarly, Fig. 8 shows the noise robustness results of the SRC and RBF kernel based SVM methods for the background

noise, which was measured by the recorded resting state. For the background noise, the noise power was controlled by scale factor α (see Eq. (5)). It was found that the classification accuracy of SRC was higher than that of the RBF SVM for all SNR cases. In addition, when the noise power increased, the accuracy difference between the SRC and SVM increased. For example, in the noiseless case, the average accuracy difference between the SVM and SRC was 1.9%. However, in the case of 0.5 and -4dB SNR, the difference was 5.8% and 8.5%. This means that the SRC method was more robust than the SVM for the polluted test signal in the background noise case.

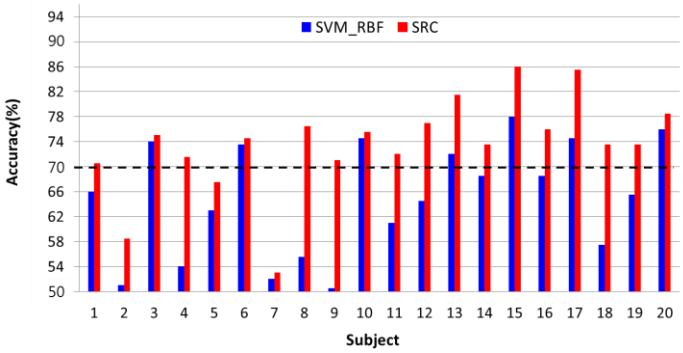

Fig. 9. Classification accuracy of RBF based SVM and SRC method for polluted test data by background noise (-4dB).

In two-class classification problems, the theoretical chance level is 50%. However, in many EEG based BCI studies [26,34,35], at least 70% classification accuracy is considered as a threshold for an acceptable communication and device control. In Fig. 9, we examine the classification performance for the polluted test data. Fig. 9 shows the classification accuracy of all subjects for the -4dB SNR for background noise cases shown in Fig. 8. The threshold of 70% classification accuracy is represented by black dotted line. For this threshold, the SVM has seven datasets that are over the threshold and the SRC has seventeen datasets. This means that for the noisy test data, 10 more subjects can use a reliable BCI system with the SRC compared to the SVM method.

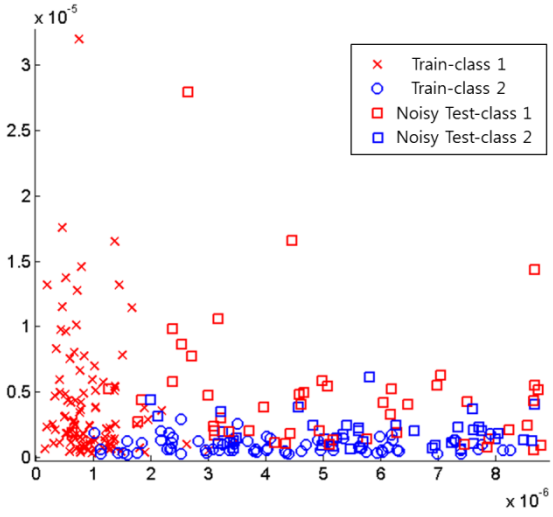

Fig. 10. Scatter plot of training data and noisy test data in two-dimensional feature space (2 CSP filters) for one subject dataset. Noisy test data are generated using background noise with 4 dB SNR.

Fig. 10 shows an example of training and polluted test features for one subject dataset. In this example, the background noise with 4 dB SNR (shown in Fig. 8) was used for the polluted test data. The positions of noisy test features (red and blue squares in Fig. 10) in two-dimensional feature space were relocated from the positions of the original training features (red x-marks and blue circles) to places with a particular direction. This represents a typical situation that occurs in real-time BCI scenario where the online test data has different background noise compared to the training data [16]. In this study, the positions of the noisy test features were varied according to the SNR of the test data.

4. Discussions

4.1. Comparison of Classification Mechanism

In this section, we examine the algorithmic difference between the SRC and SVM methods as the role of signal classification. Fig. 11 shows the classification algorithms for both methods. Feature vectors for the training data were used as an input for both classification algorithms.

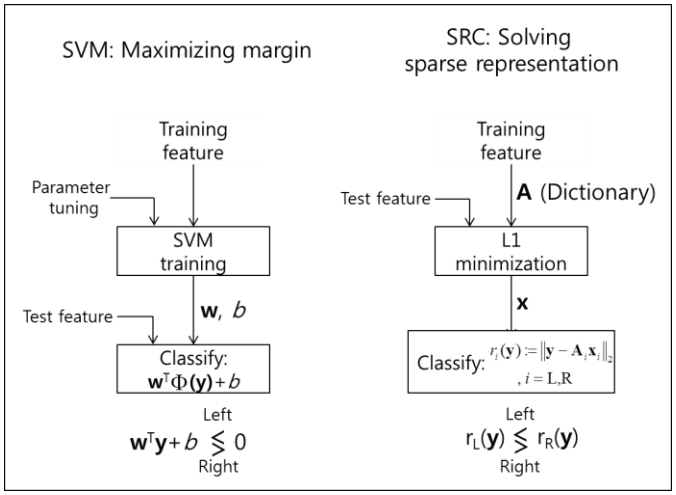

Fig. 11. Comparison of the SVM and SRC classification algorithm.

In the SVM algorithm, the input feature data and model parameters were used and the training was performed to find the parameters **w** and b for decision boundary as shown in Eq. (3). Based on the boundary, the test feature was classified. Thus, the **y** class information was determined by the decision boundary.

In the SRC algorithm, the dictionary was simply formed by collecting the input training feature vectors as the columns of the dictionary. Then, using the dictionary, sparse representation was performed for each test data. Thus, scalar coefficient vector **x** was obtained by solving L1 minimization as shown in Eq. (1). Using **x**, class information was determined by computing the residual $r(\mathbf{y})$ in Eq. (2).

Our aim was to highlight the important difference of the classification mechanism of the SRC and SVM methods as follows:

- In SVM, a fixed decision rule (decision boundary) was obtained for the entire set of training signals. Then, for each test signal, this fixed decision rule was used for signal classification.
- In SRC, the sparse representation was adaptively performed for each test signal by utilizing all training signals in the dictionary.

4.2. Robustness Analysis of SRC

The experimental results presented in section 3 shows that

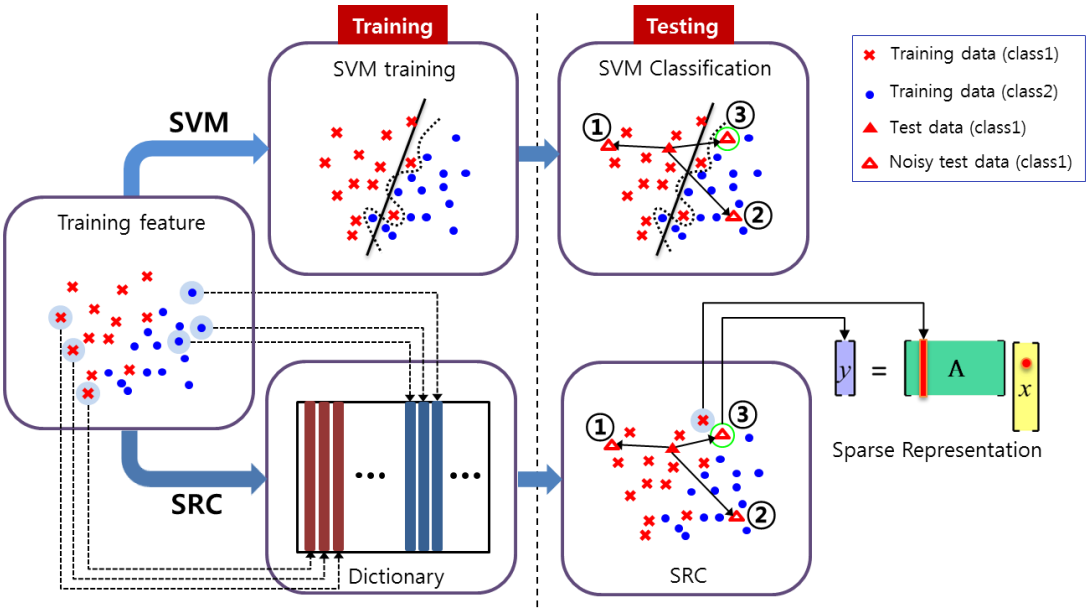

Fig. 12. Comparison of the classification procedure and characteristic of the SVM and SRC for the noisy test data. In the SVM part, black solid line and black dotted line indicate the decision boundaries for linear and RBF based SVM.

SRC had a better classification accuracy than the conventional SVM for motor imagery based EEG signal. In addition, SRC was more robust for polluted test data than SVM. In this section, we discuss the relationship between the classification performance and the difference in the classification mechanism for SRC and SVM methods.

Fig. 12 shows the concept of the classification strategy for the SVM and SRC using a toy example of polluted test data in two-dimensional feature space. In the SVM classification, decision hyperplane and non-linear decision boundary were presented for linear and RBF based SVM. For many conventional classifiers including SVM, the classifier was trained using training data; thus, the best decision rule was determined. Then, this classification rule was applied to each test data. However, as we have shown in Fig. 12, when the test data was polluted and shifted in feature space, the decision rule could not guarantee a satisfactory classification performance. On the other hand, in the SRC method, no classification rule was designed in the training part of SRC. Instead, a dictionary was formed by collecting feature vectors of the training data. Then, the sparse representation was performed for each test data using the dictionary. In addition, for the noisy test data, an independent classification task was performed in each classification by using all the training data instead of a fixed decision rule.

For a detailed analysis, we considered three possible cases of polluted test data that are presented by numbers ①, ②, and ③ in Fig. 12:

In the first case, test data was shifted away from the decision boundary and positioned at the same class feature space. In this case, both SVM and SRC correctly classified the noisy test data.

In the second case, the test data was positioned at a different class feature space of training data. Then, based on the decision boundary, the SVM classified the test data incorrectly. In the SRC method, the test data was more likely to be represented with different class training data. Thus, both classifiers were not working correctly.

Note that in the third case, similar to the second case, the test data was placed at a different class feature space. At the same time, the test data could be possibly positioned near the decision boundary. In this case, based on the decision rule obtained from the training data, the SVM resulted in wrong classification.

When we used non-linear decision boundary, e.g., RBF SVM, as shown in black dotted line, this line was optimal for the training data. Thus, the classification error could be less than the linear decision hyperplane. However, for the polluted test data, the non-linear decision boundary was fixed. On the other hand, in the third case, SRC still had a chance for correct sparse representation with the same class training data as shown in Fig. 12. This was possible because the SRC method did not depend on a fixed decision rule that was obtained from the training data. Instead, for each classification of test data, the SRC method directly used all training data and performed sparse representation.

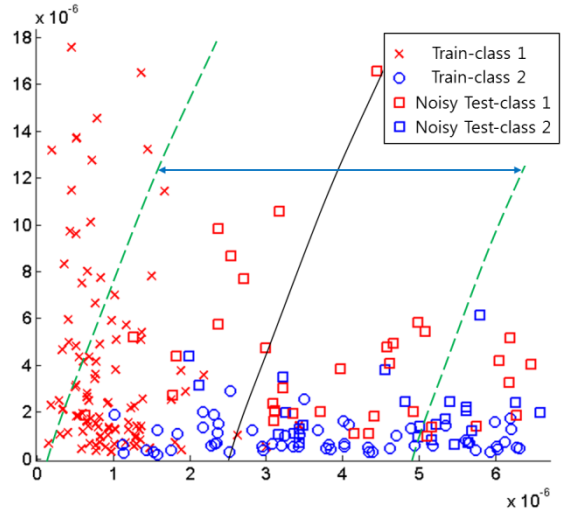

Fig. 13. Scatter plot of training data and noisy test data in two-dimensional feature space (2 CSP filters) for one subject data. Noisy test data are generated using background noise with 4 dB SNR.

To evaluate the validity of our analysis, we examined the same data shown in Fig. 10 in details. Fig. 13 shows an enlarged version of the scatter plot using the training and noisy test data. The black line indicates the obtained decision boundary from the RBF kernel based SVM. The region between the two green

dotted lines is chosen as the near area of the decision boundary. In this area, many miss-classification cases may occur for both classifiers. In addition, most of the polluted test data, which correspond to case ③ in Fig. 12 are located in this region.

For all noisy test data (i.e., 100 trials), the RBF SVM and SRC showed the classification accuracy of 56% and 62%, respectively. Because we used only two CSP filters for visualization, the classification accuracy was very low compared with the results given in Fig 8.

For the noisy test data, which are located between the green dotted lines, the RBF SVM showed 57% classification accuracy. However, the SRC showed an improved classification accuracy of 83%. In addition, when we only considered the noisy test data for case ③ examples, the RBF SVM had 18 miss-classification data. However, the SRC correctly classified 12 test data among 18 test data. Therefore, we confirmed that the noisy test data of case ③ were miss-classified from the fixed rule based SVM. On the other hand, for the same data, the SRC correctly classified many times with the effort of independent classification task for each test data using all training data.

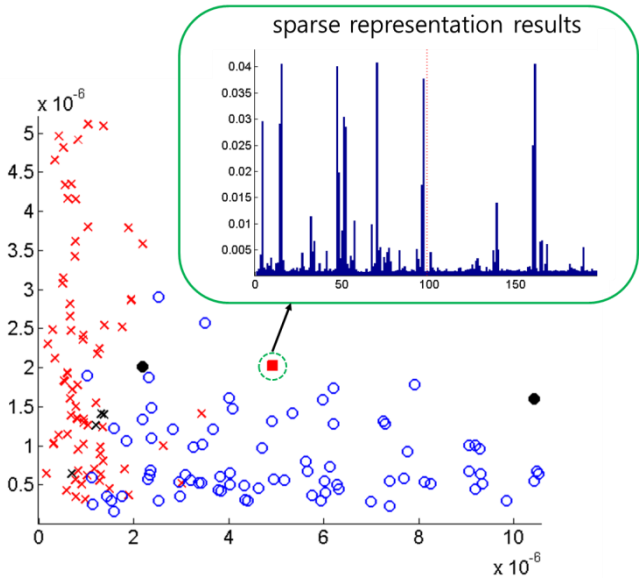

Fig. 14. Scatter plot of training data and noisy test data. The figure inside the green box indicates the sparse representation result of the noisy test data.

Fig. 14 shows one instance of the noisy test data that was not correctly classified by the SVM; however, was correctly classified by the SRC method. The test signal of class 1 is represented by a red square, which is located in the region between the green dotted lines shown in Fig. 13. The figure inside the green box shows the recovered coefficient **x** from the SRC method. Using the trial numbers (x-axis of the figure inside the green box) with large coefficient values, we represented the corresponding trials by the black x-marks and circles in Fig. 14. Four largest coefficient values were selected for class 1. Two largest coefficient values were selected for class 2. As it can be seen, the noisy test trial of class 1 (red square) is located near the training trials of class 2. However, in the SRC method, using the coefficient **x,** the test trial could be correctly classified from the minimum residual rule in Eq. (2). In addition, in each test trial, a different coefficient **x** which represented the test data most compactly, was recovered by L1 minimization. Therefore, for the case of time varying EEG signal classification, the SRC approach was much more appropriate to employ than the SVM method, which was based on the fixed decision rule.

An adaptive classification scheme for a conventional classifier such as LDA and SVM was studied to overcome the non-stationary problem of EEG signals [16,27,41]. In the adaptive techniques, typically decision boundary was updated (relearned) using collected labeled test data for a given duration. However, after designing new decision boundary, new test signal was dependent to the decision boundary. Thus, the adaptive scheme for the conventional classifier was still a decision rule based classification. Therefore, it could not be adaptively applied to each test signal. We think that some adaptation techniques for SRC [30–31], i.e., dictionary learning using collected signals, can be more efficient for real-time online BCI systems. Therefore, the comparison of the adaptive classification schemes between the SRC and conventional classifier is an interesting area for our future research.

4.3. Computation Time Analysis

In this section, we evaluate the computation time (running time) of the classification algorithms for the experimental datasets.

As it can be seen in Fig. 12, the most time consuming process of the SVM occurred while training the SVM. On the other hand, the most computation cost in the SRC algorithm occurred in L1 minimization step for sparse representation. Therefore, our evaluation for running time focused on the SVM training and L1 minimization step for the SRC algorithm. We used the *tic* and *toc* MATLAB commands to measure the start and end time of the SVM and SRC algorithms, respectively. We simulated all algorithms in the same environment using MATLAB 7.14 (R2012a) with 3.30 GHz processor and 8 GB memory.

For a single test trial, the average computation time for the SVM and SRC was 12.1 msec and 16.7 msec respectively. This computation time was averaged for 100 test trials of all subjects. However, in the case of online BCI classification, typically the SVM decision boundary was designed once using the training data. Then, all the test data was classified based on the decision boundary. On the other hand, independent classification task was performed for each test data in the SRC. Therefore, the computation time of the SRC method increased by the number of test trials. Thus, a robust classification performance of SRC included the cost of the computation time at each test trial.

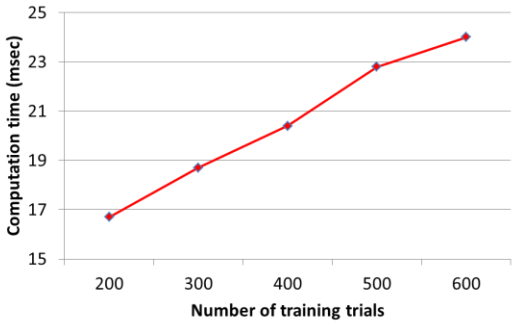

Fig. 15. Computation time of the SRC as a function for the number of training trials.

In this study, the size of the dictionary, i.e., the number of training trials, was 200. In this case, the computation time of the SRC was very small and negligible (16.7 msec). In addition, in Fig. 15, we display the average computation time as a function of the number of training trials. When the size of dictionary was increased, the difference of the computation time was just a few milliseconds. Therefore, this was not an important factor for an online classification in BCI systems. In addition, recently developed fast L1 minimization algorithms were used for the SRC method. In [24], authors showed that a few of the fast L1 minimization algorithms provided faster computation time than the conventional SRC method for large datasets of real face images.

Note that even though the computation time of the SVM was smaller than the SRC, the SVM required more effort to select a proper kernel and tune the model parameters for accurate classification results [6,25].

4.4. Online Data Analysis

In this study, we modeled noisy test data by adding two noise sources into the original trial data and controlled the noise power to evaluate the noise robustness of the SRC systematically. In this section, we aim to evaluate the SRC using online motor imagery experimental dataset. In this experiment, the training session and online test session were independently performed. Thus, in this evaluation, we used a non-stationary dataset from an online motor imagery experiment.

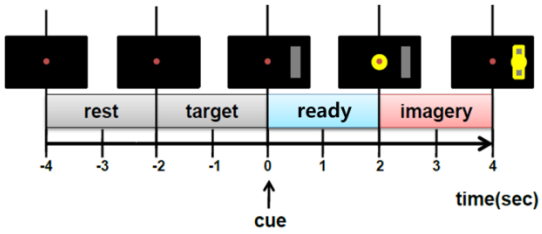

Fig. 16. Single trial procedure for online motor imagery experiment.

Five subjects participated in our online experiment. Right hand (R) and foot (F) motor imagery were performed for each subject. The sampling rate of these datasets was 512 samples per second, and the number of EEG channels was 64. The detailed experimental paradigm is illustrated in Fig. 16. The same paradigm was used for both training (calibration) and online testing (feedback) sessions. In each trial, the target bar was presented on 0 sec at the right or left side of the screen corresponding to the right or foot motor imagery. Two seconds after cue onset, the subject was instructed to perform the motor imagery task. During the training session, no feedback was provided. However, in the online testing session, the online feedback was provided in each trial. We collected 60 training trials and 75 online test trials for each class. After data segmentation from 2 to 4 sec, we performed the same preprocessing step that was used in section 2.2.

As shown in Fig. 17, using five online datasets, we evaluated the classification accuracy of the SRC and SVM_RBF. Even though size of the online dataset was small compared with the twenty offline datasets used in Fig. 5, we obtained consistent results. Thus, the SRC showed better mean classification accuracy than the SVM for the online datasets. Except one subject's dataset, which showed the same accuracy, the classification accuracy of the SRC was better than the SVM_RBF method for four subjects.

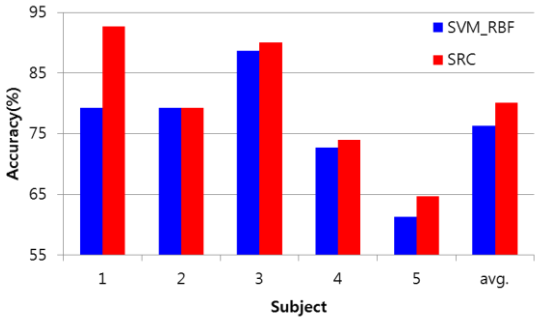

Fig. 17. Comparison of the classification accuracy of the SRC and SVM_RBF for online experimental dataset.

5. Conclusions

In this paper, we evaluated and analyzed the robustness of the SRC method against the non-stationarity of EEG signal classification. For this purpose, we generated noise corrupted EEG test signals using two noise sources such as random Gaussian noise and scalp recorded background noise. Then, we assessed the classification performance of the SRC when the noise power was varied. Using the experimental motor imagery based EEG and generated noisy test signals, we compared the classification results of the SRC with that of the SVM method, which has been considered as a robust classifier in many BCI studies. From the results, it was evident that the SRC showed superior noise robustness than the SVM for both Gaussian and background noise. Furthermore, the results of the online-experimental dataset showed that the classification accuracy of the SRC was better than the SVM. We analyzed that the robust classification accuracy of the SRC was due to a different classification approach compared with the conventional decision rule based SVM. Thus, the SRC showed an inherent adaptive classification mechanism for each test trial via optimal sparse representation of the training trials. In addition, we showed that the computation time of the SRC for a robust classification was on the order of milliseconds, which was acceptable for real time BCI systems.

Acknowledgments

This work was supported by the National Research Foundation of Korea (NRF) grant funded by the Korean government (MEST) (Do-Yak Research Program, No. 2010-0017944).

References

[1] Wolpaw, J.R. Birbaumer, N., McFarland, D.J., Pfurtscheller, G., Vaughan, T.M., 2002. Brain-computer interfaces for communication and control. Clin. Neurophysiol. 113 (6), 767–791.

[2] Sellers, E., Donchin, E., 2006. A P300-based brain-computer interface: Initial tests by ALS patient. Clin. Neurophysiol. 117 (3), 538–548.

[3] Pfurtscheller, G., Flotzinger, D., Kalcher, J., 1993. Brain-computer interface-a new communication device for handicapped persons. J. Microcomput. Appl. 16 (3), 293–299.

[4] Wolpaw, J.R., McFarland, D.J., Neat, G.W., Forneris, C.A., 1991. An EEG-based brain-computer interface for cursor control. Electroencephalogr. Clin. Neurophysiol. 78 (3), 252–259.

[5] Ramoser, H., Müller-Gerking, J., Pfurtscheller, G., 2000. Optimal spatial filtering of single trial EEG during imagined hand movement. IEEE Trans. Rehabil. Eng. 8 (4), 441–447

[6] Lotte, F., Congedo, M., Lecuyer, A., Lamarche, F., Arnaldi, B., 2007. A review of classification algorithms for EEG-based brain-computer interfaces. J. Neural Eng. 4 (2), R1–R13.

[7] Dornhege, G., del, R. Millán J., Hinterberger, T., McFarland, D.J., Müller, K.R., 2007. Toward Brain-Computer Interfacing, The MIT Press, pp. 213–215.

[8] Huang, K., Aviyente, S., 2006. Sparse representation for signal classification. Adv. Neural Inf. Process. Syst. 19**,** 609–616.

[9] Wright, J., Yang, A.Y., Ganesh, A., Sastry, S.S., Ma, Y., 2009. Robust face recognition via sparse representation. IEEE Trans. Pattern Anal. Mach. Intell. 31 (2), 210–227.

[10] Gemmeke, J.F., Virtanen, T., Hurmalainen, A., 2011. Exemplar-based sparse representations for noise robust automatic speech recognition. IEEE Trans. Audio, Speech, Lang. Proc. 19 (7), 2067–2080.

[11] Younghak, S., Seungchan, L., Junho, L., Heung-No, L., 2012. Sparse representation-based classification scheme for motor imagery-based brain-computer interface systems J. Neural Eng. 9, 056002.

[12] Yang, M. and Zhang, L., 2010. Gabor Feature based Sparse Representation for Face Recognition with Gabor Occlusion Dictionary. In ECCV.

[13] Wright, J., Ma, Y., Mairal, J., Sapiro, G., Huang, T., and Yan. S., 2010. Sparse representation for computer vision and pattern recognition. Proceedings of IEEE, Special Issue on Applications of Compressive Sensing & Sparse Representation, 98(6):1031-1044.

[14] Schlögl, A., Lee, F., Bischof, H., Pfurtscheller, G., 2005. Characterization of four-class motor imagery EEG data for the BCI-competition. J. Neural Eng. 2 (4), L14–L22.

[15] Kaper, M., Meinicke, P., Grossekathoefer, U., Lingner, T., Ritter, H., 2004. BCI Competition 2003--Data set IIb: support vector machines for the P300 speller paradigm. IEEE Trans. Biomed. Eng. 51 (6), 1073-1076.

[16] Shenoy, P., Krauledat, M., Blankertz, B., Rao, R.P.N., Müller, K.-R., Towards adaptive classification for BCI J. Neural Eng., 3 (2006), pp. R13–R23

[17] Donoho, D.L., 2006. Compressed sensing. IEEE Trans. Inf. Theory 52 (4), 1289–1306.

[18] Baraniuk, R., 2007. Compressive sensing. IEEE Signal Process. Mag. 24 (4), 118–121.

[19] Sergios, T., Aggelos, P., Konstantinos, K., Dionisis, C., 2010. Introduction to Pattern Recognition :A Matlab Approach, Academic Press, 43–57.

[20] Blankertz, B., Tomioka, R., Lemm, S., Kawanabe, M., Müller, K-R., 2008. Optimizing spatial filters for robust EEG single-trial analysis. IEEE Signal Process. Mag. 25 (1), 41–56.

[21] Candès, E., Romberg, J., Tao, T., 2006. Stable signal recovery from incomplete and inaccurate measurements. Comm. Pure Appl. Math. 59 (8), 1207–1223.

[22] Wasserman, L., 2010. All of Statistics: A Concise Course in Statistical Inference, Springer, 63–64.

[23] MathWorks: http://www.mathworks.co.kr/kr/help/stats/support-vector-machines-svm.html

[24] Yang, A.Y., Zhou, Z., Ganesh, A., Sastry, S.S., Ma, Y., 2013. Fast l1-minimization algorithms for robust face recognition. IEEE Trans. Image process. 22 (8), 3234–3246.

[25] Hsu, C.-W., Chang, C.-C., and Lin, C.-J. 2003. A practical guide to support vector classification. Tech. rep., Department of Computer Science, National Taiwan University.

[26] Kübler, A., Neumann, N., Wilhelm, B., Hinterberger, T., Birbaumer, N., 2004. Predictability of brain–computer communication. J Psychophysiol. 18:121–129.

[27] Oskoei, M.A., Gan, J.Q., Huosheng, H., 2009. Adaptive schemes applied to online SVM for BCI data classification, Inter. Conf. IEEE on Eng. in Medicine and Biology Society (EMBC), 2600-2603

[28] Yu, H., Lu, H., Ouyang, T., Liu, H., and Lu, B. L., 2010 Vigilance detection based on sparse representation of EEG Proc. 32nd Annual Int. Conf. of the IEEE Engineering in Medicine and Biology Society, 2439–42

[29] Blanchard, G., and Blankertz, B., 2004 Bci competition 2003-data set iia: spatial patterns of self-controlled brain rhythm modulations. IEEE Transactions on Biomedical Engeneering, 51(6):1062-1066.

[30] Aharon, M., Elad, M., and Bruckstein, A., 2006 K-svd: An algorithm for designing overcomplete dictionaries for sparse representation. IEEE Trans. Signal Process., 54 (11), 4311-4322.

[31] Yang, M., Zhang, L., Feng, X., and Zhang, D., 2011 Fisher discrimination dictionary learning for sparse representation. IEEE International Conference on Computer Vision, 543-550.

[32] Sanei, S., Chambers, J. A., 2007 EEG Signal Processing (John Wiley & Sons Inc.)

[33] Morioka, H., Kanemura, A., Hirayama, J.-I., Shikauchi, M., Ogawa, T., Ikeda, S., Kawanabe, M., and Ishii, S., 2015 Learning a common dictionary for subject-transfer decoding with resting calibration. NeuroImage, 111, 167-178.

[34] Sellers, E. W., Kubler, A., Donchin, E., 2006 Brain-computer interface research at the University of South Florida Cognitive Psychophysiology Laboratory: the P300 Speller IEEE Trans Neural Syst Rehabil Eng, 14(2), 221–224.

[35] Yang, L., Leung, H., Peterson, D. A., Sejnowski, T. J., Poizner, H., 2014 Toward a Semi-Self-Paced EEG Brain Computer Interface: Decoding Initiation State from Non-Initiation State in Dedicated Time Slots. PLoS ONE 9(2): e88915.

[36] Blankertz, B., Kawanabe, M., Tomioka, R., Hohlefeld, F., Nikulin,V., Müller, K. R., 2008 Invariant common spatial patterns: Alleviating nonstationarities in brain–computer interfacing. Platt, J., Koller, D., Singer, Y., Roweis, S., (Eds.), Advances in Neural Information Processing Systems 20, MIT Press, Cambridge, MA, 113–120.

[37] Hohyun, C., Minkyu, A., Santae, A. and Sung, C., J., 2013 Strategy for Reducing Calibration Time With Invariant Common Spatio-Spectral Patterns. Proceedings of the fifth international brain-computer interface meeting, ID 123, 2013.

[38] Samek, W., Vidaurre, C., Müller, K. R. and Kawanabe, M., 2012 Stationary common spatial patterns for brain-computer interfacing. J. Neural Eng., 9(2), 026013.

[39] Arvaneh, M., Guan, C., Ang, K., K. and Quek, C., 2013 Optimizing spatial filters by minimizing within-class dissimilarities in electroencephalogram-based brain-computer interface. IEEE Trans. Networks and Learning Sys, 24(4), 610-619.

[40] Kawanabe, M., Samek, W., Müller, K. R. and Vidaurre, C., 2014 Robust common spatial filters with a maxmin approach. Neural Comput., 26(2), 1-28.

[41] Vidaurre, C., Kawanabe, M., von Bünau, P., Blankertz, B. and Müller, K. R., 2011 Toward unsupervised adaptation of LDA for brain–computer interfaces IEEE Trans. Biomed.Eng. 58, 587–597.

[42] Billinger, M., Brunner, C. and Müller-Putz G., R., 2013 Single-trial connectivity estimation for classification of motor imagery data, J. Neural Eng., 10(4), 046006.